

## FRACTURE MECHANICS OF AXIAL - SYMMETRICAL BIMETALS

N. A. Mackhutov, A. I. Tananov, N. N. Avtonomov and G. A. Slavkin

*Engineering Mechanical Research Institute, Moscow, USSR*

### ABSTRACT

Theoretical and experimental studies have been made on axial - symmetrical bimetal (ЭМ 69-У7) specimens containing different depth incisions and cracks of ring form. The strain intensity factors for bimetal specimens, taking into consideration different levels of the random stress state at crack tip and in dangerous cross section have been studied. The fracture toughness of bimetal specimens is also discussed.

### INTRODUCTION

Axial - symmetrical bimetal composites (ABM) are widely used for row-shafts of sea ships, cutting tools, flexible shafts, etc. The estimation of the usability ABM composed of high strength steel (core) and mild steel (cover) for bolts, hairpins and another components having high stress concentration is significant problem. Analytical and experimental methods of fracture toughness determination for sheet-type bimetal under static and cyclic loads are widely developed, but reported data about strain peculiarities and strength characteristics are limited. There is especially a lack of data about ABM under nonhomogeneous stress state and elasto-plastic deformation.

### RESULTS OF THEORETICAL AND EXPERIMENTAL STUDIES

Theoretical and experimental studies have been made on ABM-specimens, which consist of cover layer - CrNiW steel and core layer - У7 steel with  $d_c/D = 0,5$  ( $d_c$  - core diameter,  $D$  - cover diameter).

The " $\sigma - e$ " curves of several special zones of ABM were used for describing of deformation processes of bimetal (in relative stresses  $\bar{\sigma}_n = \sigma_n/\sigma_r$  and strains  $\bar{e}_n = e_n/e_r$ ). The " $\sigma - e$ " curves are described both linear

$$\bar{\sigma} = \bar{e} \quad \text{for} \quad \bar{e} \leq 1; \quad \bar{\sigma} = 1 + \bar{\sigma}_r(\bar{e} - 1) \quad \text{for} \quad \bar{e} > 1 \quad (1)$$

and power functions

$$\bar{\sigma} = \bar{e} \quad \text{for } \bar{e} \leq 1; \quad \bar{\sigma} = \bar{e}^m \quad \text{for } \bar{e} > 1 \quad (2)$$

Then conditional yield strengths of  $j$ -part curve " $\sigma - e$ " are presented as:

$$\sigma_{Tj} = \left[ \sum_{j=1}^k F_j \sigma_j(e_{Tj}) \right] / \left[ \sum_{j=1}^k F_j \right] \quad (3)$$

where:  $\sigma_j(e_{Tj})$  - stress values taking from curves " $\sigma - e$ " for the components of material under strain  $e_{Tj}$ , which correspond to yield strength of  $j$ -material;  $F_j$  - area under every curve " $\sigma - e$ ".

A linear hardening coefficient  $\bar{G}_{Tj}$  of  $j$ -part of material is

$$\bar{G}_{Tj} = [(\sigma_{T(j+1)} / \sigma_{Tj}) - 1] / [(e_{T(j+1)} / e_{Tj}) - 1] \quad (4)$$

$$m_j = [\lg(\sigma_{T(j+1)} / \sigma_{Tj})] / [\lg(e_{T(j+1)} / e_{Tj})] \quad (5)$$

The stress-strain field determinations are an important problem under investigation of bimetallic pivot elements with ring concentrators and cracks.

Neuber's solutions (Neuber, 1944) for deep and small incisions on the rotation body were used in elastic field for single material pivot. The stress condition is characterized for intermediate depth incisions by means of the stress concentration factors, which is obtained by interpolation

$$\alpha_{\sigma_1} = \frac{\sigma_1}{\sigma_n^m} = 1 + \frac{(\alpha_1^q - 1)(\alpha_1^m - 1)}{\sqrt{(\alpha_1^q - 1)^2 + (\alpha_1^m - 1)^2}}; \quad (6)$$

$$\alpha_{\sigma_2} = \frac{\sigma_2}{\sigma_n^m} = \frac{\alpha_2^q \cdot \alpha_2^m}{\sqrt{(\alpha_2^q)^2 + (\alpha_2^m - 1)^2}}$$

where:  $\alpha_{\sigma_1}$ ,  $\alpha_1^q$ ,  $\alpha_1^m$ ,  $\alpha_{\sigma_2}$ ,  $\alpha_2^q$ ,  $\alpha_2^m$  - stress concentration factors of first ( $\sigma_1$ ) and second ( $\sigma_2$ ) main stresses, for intermediate and small incisions respectively.

Now introduce stress concentration factors for deep and small incisions based on net section nominal stresses

$$\sigma_{n\xi}^n = \sigma_{j\xi}^n / \alpha_{\sigma_n}; \quad \alpha_{j\xi}^q = \sigma_{j\xi}^q / \sigma_n^q; \quad \alpha_{j\xi}^m = \sigma_{j\xi}^m / \sigma_n^m \quad (j=1, 2, 3) \quad (7)$$

where:  $\xi = r/a$  - relative coordinate for intermediate depth incision.

By substitution of (7) in (6), we derive formulae for calculations of the stresses in net-section of intermediate depth incision

$$\sigma_{1\xi} = \sigma_n^m \left[ 1 + \frac{(\sigma_{1\xi}^q - \sigma_n^q)(\sigma_1^m - \sigma_n^m)}{\sqrt{(d/D)^4 (\sigma_{1\xi}^q - \sigma_n^q)^2 + (\sigma_1^m - \sigma_n^m)^2}} \right];$$

$$\sigma_{2\xi} = \frac{\sigma_n^q \sigma_{2\xi}^q \sigma_{2\xi}^m}{\sqrt{(d/D)^4 (\sigma_{2\xi}^q)^2 + (\sigma_{2\xi}^m)^2}}; \quad \sigma_{3\xi} = \frac{\sigma_n^q \sigma_{3\xi}^q \sigma_{3\xi}^m}{\sqrt{(d/D)^4 (\sigma_{3\xi}^q)^2 + (\sigma_{3\xi}^m)^2}} \quad (8)$$

Finite - element method (FEM) calculation would enable us to define more precisely the solution (8) by means of coefficient  $\xi^3$  under the stresses  $\sigma_2^q$  and  $\sigma_3^q$ . This more accurate definition led to better agreement of  $\sigma_2^q$ ,  $\sigma_3^q$  with  $\sigma_2^q$ ,  $\sigma_3^q$ , respectively.

Calculations of stiffness stress state parameters in net - section  $\alpha_n$ ,  $\beta_n$  and in maximal section  $\alpha_{max}$ ,  $\beta_{max}$

$$\alpha_n = \sigma_{2n} / \sigma_{1n}; \quad \beta_n = \sigma_{3n} / \sigma_{1n}; \quad \alpha_{max} = \sigma_{2max} / \sigma_{1max}; \quad \beta_{max} = \frac{\sigma_{3max}}{\sigma_{1max}} \quad (9)$$

and of first main stress increase factors

$$\bar{I}_n = (2 / [(1 - \alpha_n)^2 + (1 - \beta_n)^2 + (\alpha_n - \beta_n)^2])^{1/2};$$

$$\bar{I}_{max} = (2 / [(1 - \alpha_{max})^2 + (1 - \beta_{max})^2 + (\alpha_{max} - \beta_{max})^2])^{1/2} \quad (10)$$

were executed on the basis of suggested method for cylindrical specimen  $D = 15$  mm containing some incisions (incision tip radius is  $\rho = 0,01$  mm and relative depth is  $0,2 < d/D < 1,0$ ), as modelling ring crack.  $I_n$  and  $I_{max}$  as function of  $d/D$ , are down - like curves with maximum under  $d/D = 0,65$  for  $I_n = 2,2$  and  $d/D = 0,5$  for  $I_{max} = 2,5$ .  $I_n$  and  $I_{max}$  were used to determine deformation fracture factors - strain intensity factors.

To evaluate stress and strain fields in elasto-plastic state we used the Neuber-Mackhutov (Mackhutov, 1981) approach, based on dependance between theoretical stress concentration factor  $K_\sigma$  and strain concentration factor  $K_\epsilon$  in elasto-plastic conditions

$$\frac{K_\epsilon K_\sigma}{\alpha_\sigma^2} = F[\alpha_\sigma, \bar{\sigma}_n, f(\bar{\sigma}_n, \bar{e}_n)] \quad (11)$$

Introduce solutions  $K_\epsilon(\xi)$  and  $K_\sigma(\xi)$  depending on the cross section coordinate

$$K_\epsilon(\xi) = \bar{e}_i(\xi) / \bar{e}_{in}; \quad K_\sigma(\xi) = \bar{\sigma}_i(\xi) / \bar{\sigma}_{in} \quad (12)$$

Nominal stress and strain intensities ( $\bar{\sigma}_{in}$  and  $\bar{e}_{in}$ , respectively) were evaluated outside concentration zones with taking into account of 3D - stress state in the concentration zone.

To receive the distribution of main stresses on net - section we made assumption that stress state stiffness parameters  $\alpha$  and  $\beta$  in elastic and elasto-plastic deformation stages are constant.

In pivot axial - symmetrical bimetal elements design (Fig. 1a) we made an assumption about continuity and equivalency of elas-

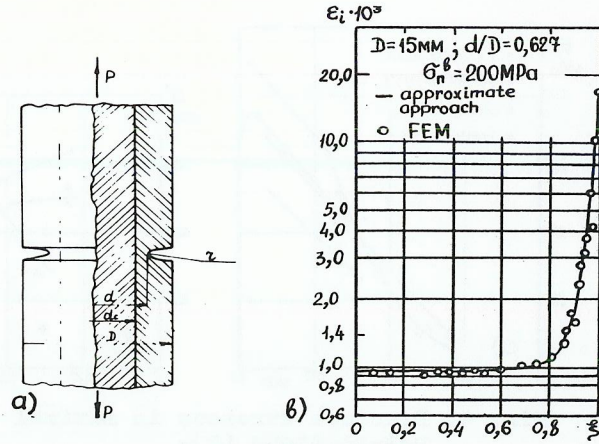


Fig. 1. Calculation scheme of the ABM-specimen containing ring incision (a) and distribution of the elasto-plastic strain intensity (b) in net-section for this case.

to-plastic strain intensity distribution  $\epsilon_i (\xi)$  on dangerous sections in bimetallic and monometallic.

Using formulae (3)-(5) and values  $\epsilon_i (\xi)$ , we received values  $\sigma_1 (\xi)$ ,  $\sigma_2 (\xi)$ ,  $\sigma_3 (\xi)$ . Strain intensity distribution with FEM - solution results (Fig. 1b). Distributions of elasto-plastic main stresses in a dangerous section are presented in Fig. 2.

The created procedure for stress and strain fields calculation in ABM - specimens give a possibility to evaluate limit state in concentration zone and critical stress values for bimetallic pivot elements.

Ultimate failure strain intensity  $\epsilon_{ic}$  was taken as fracture criteria. Nominal strain intensity  $\epsilon_{inc}$  for specimen with stress concentration is connected with fracture strain for smooth specimen:

$$K_e \cdot \epsilon_{inc} \cdot I_n / D_{en} = \epsilon_{ic} \cdot D_{emax} / I_{max} \quad (13)$$

where:  $D_{en}$  - failure plastic strain decreasing factor

$$D_{en} = \frac{K_D}{I_n (1 + \alpha_n + \beta_n)}$$

$K_D$  - material characteristic.

Relation for  $D_{emax}$  is the same as for  $D_{en}$  taking into account of  $\alpha_{max}$  and  $\beta_{max}$ .

If the nominal failure stress intensity  $\sigma_{inc}$  exceed the yield strength, equation (13) can be represented with taking into account of resistance increase to plastic strains due to 3D-stress state

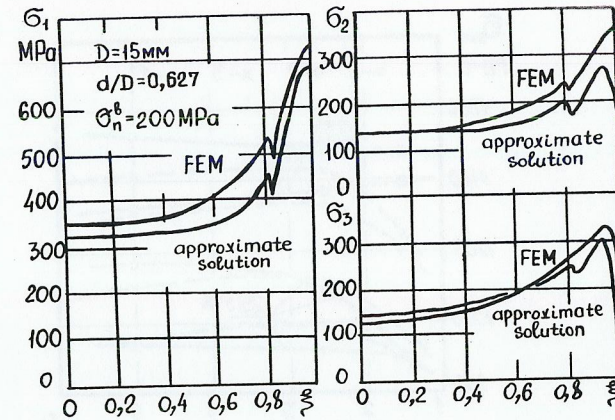


Fig. 2. Distribution of the elasto-plastic stresses in a dangerous section.

$$\bar{\sigma}_{inc} / \bar{\sigma}_e = (I_{max} / I_n)^{1-m} (D_{emax} / D_{en} / K_e)^m \quad (14)$$

The results of the calculations by (14) and experimental data for single-metallic and bimetallic cylindrical pivot specimens ( $D = 15$  mm) containing ring incisions  $\alpha_e = 1,5; 2,5; 5,0$ . Are presented on Fig. 3. The curves on the Fig. 3 present a good agreement with calculation and experimental results.

The study of the limit state for specimens containing cracks was conducted on the basis of strain intensity factor theory (Mackhutov, 1981), taking into account 3D-stress state in a dangerous section and in a crack tip.

The expressions of critical strain intensity factor for fracture stage (index  $n$  and  $m$  reflect effect of  $I_n$  and  $I_{max}$  respectively) are:

$$\bar{K}_{rec}^{nm} = \left( \frac{K_e^*}{\bar{\sigma}_{0,2} I_{max}} \right)^{P_{ke}} \quad \text{for } \sigma_{nc} \leq \bar{\sigma}_{0,2} I_n \quad (16)$$

$$\bar{K}_{rec}^{nm} = \left( \frac{\sigma_{nc}}{\bar{\sigma}_{0,2} I_n} \right)^{n_g} \left( \frac{K_e^*}{\bar{\sigma}_{0,2} I_{max}} \right)^{P_{ke}} \quad \text{for } \sigma_{nc} > \bar{\sigma}_{0,2} I_n$$

where:  $P_{ke}$ ,  $n_g$  - material characteristics and load conditions.

The experimentally received functions for " $\sigma_n - V$ " ( $\sigma_n$  - nominal stress in net-sections;  $V$  - crack opening displacement) with taking into account (16) for  $\bar{K}_{re}$  are

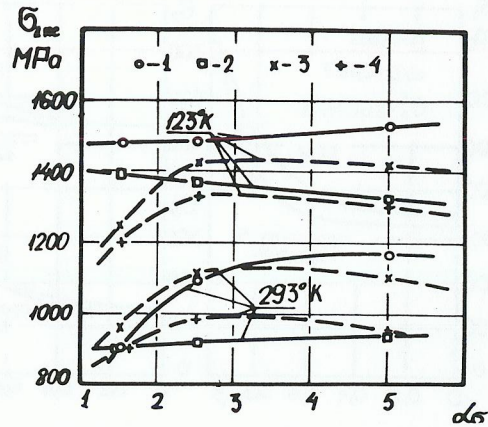


Fig. 3. Failure stresses  $\sigma_{inc}$  for incision specimens as a function of theoretical concentration factor (ABM: 1 - experiment; 3 - calculation.  $\Sigma\text{И-69}$ : 2 - experiment; 4 - calculation).

$$V = V_e \text{ for } \bar{\sigma}_n < 0,7 I_n \sigma_T; V = V_e \left( \frac{\sigma_n}{0,7 I_n \sigma_T} \right)^{p_{ke}} \text{ for } 0,7 < \frac{\bar{\sigma}_n}{I_n} < 4,0$$

$$V = V_e \left( \frac{\sigma_n}{I_n \sigma_T} \right)^{n_g} \left( \frac{\sigma_n}{0,7 I_n \sigma_T} \right)^{p_{ke}} \text{ for } \bar{\sigma}_n > I_n \quad (17)$$

The curves " $\sigma_n - V$ " have good agreement with experimental one's for monometals. However, the calculated and experimental curves for bimetal have some divergency because of dividing bimetal on layers in some cases.

The fracture toughness tests of cylindrical specimens under static loading were conducted with the recording "P - V" and "P - f" plots (P - load, V - crack opening displacement, f - load-line displacement) at the temperatures from 103 K to 293 K.

The analysis of power (Fig. 4) and energy fracture criteria shows that the bimetal has advantage vs  $\Sigma\text{И-69}$  and  $\gamma 7$  steels in the range of  $0,65 < d/D < 1,0$  both at the room and low temperatures. This tendency is increased under low (103 K) temperatures.

Studies of strain intensity factors  $\bar{K}_{rec}$ ,  $\bar{K}_{rec}^n$  and  $\bar{K}_{rec}^{nm}$  which take into consideration the 3D - stress state in different way show that the factor  $\bar{K}_{rec}^{nm}$  is the most stable characteristic in respect to crack lengths (Fig. 5).

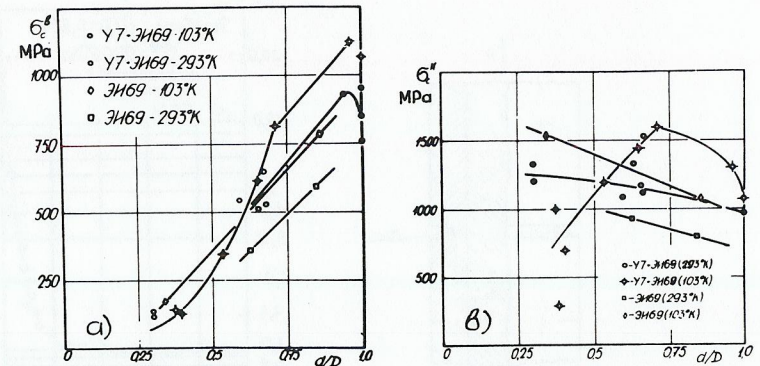


Fig. 4. Fracture stresses in maximal - (a) and net-sections (b).

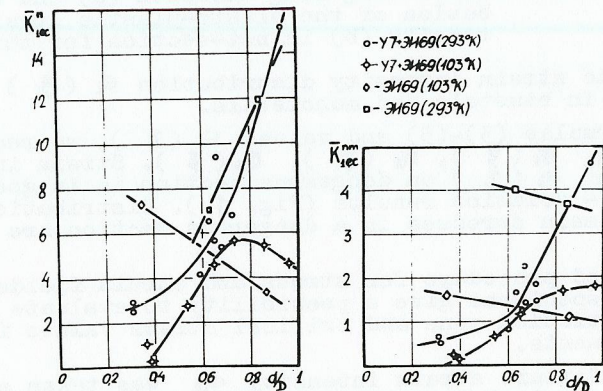


Fig. 5. The effect of 3D - stress state on strain intensity factors.

REFERENCES

Neuber, G. (1947). Concentratia naprijazeni, M-L, Gostechizdat, 204 s.  
 Mackhutov, N.A. (1981). Deformacionnie criteri razrusheniya i raschet elementov constructii na prochnost, M. Mashinostroyeniye, 272 s.